

Electron reconstruction and identification in ATLAS. Implication for the Higgs into four electron final state.

Fany DUDZIAK

on behalf of the ATLAS Collaboration

Laboratoire de l'Accelérateur Lineaire, Université Paris XI, Orsay

The Higgs boson search is one of the primary challenges at the LHC and especially for the ATLAS experiment. The golden Higgs boson decay to four leptons, $H \rightarrow ZZ^* \rightarrow 4l$, is one of the most promising discovery channels. Because of the small cross-section, a high electron reconstruction efficiency is required, especially for a low mass standard Higgs boson. The baseline analysis for the $H \rightarrow ZZ^* \rightarrow 4e$ search and the latest optimizations performed for the electron reconstruction are described.

1 Introduction

The Higgs mechanism predicts the existence of a scalar particle in the Standard Model: the Higgs boson. Elementary particles generate their mass by interacting with the Higgs boson. For the vector bosons this interaction is breaking the electroweak symmetry. The Higgs boson search was carried out for many years at LEP and currently at the Tevatron without discovery⁴. In ATLAS it will be hunted for in several decay channels, particularly in the ZZ^* to four leptons channel. This channel takes advantage of a very clean signal of four isolated charged leptons in the busy hadronic environment of the LHC. Robust reconstruction and performant identification of the electrons are crucial to optimize the discovery potential in this channel, especially for the low transverse momentum region which is important for a low mass Higgs boson.

2 The electron reconstruction in ATLAS

Two sub-detectors are mainly used to reconstruct electrons in ATLAS. Tracks are reconstructed by the Inner Detector operating inside the two Tesla solenoid magnet and composed of the following sub-detectors: three-layers of pixels, four double layers of silicon strips (SCT) and the transition radiation tracker (TRT). Then the liquid argon electromagnetic calorimeter measures the energy in three longitudinal layers, with a presampler layer in front. The first layer is made of strips and has the finest segmentation in η to separate photon from π^0 decays. The second layer has a coarser segmentation (e.g. 8 times the first layer in η) and contains most of the shower energy. The third layer ensures the measurement of the shower tail.

The reconstruction starts with a sliding window algorithm which aims to find electromagnetic clusters with a threshold $E_T > 3$ GeV. When a cluster seed is found, one looks for a track pointing to it. In the case of a good track-cluster match, the cluster is considered an electron and calibrated as such. Otherwise it is calibrated as a photon. Because of bremsstrahlung

the electron clusters are wider in ϕ for better containment in the magnetic field, and photon clusters are somewhat narrower in ϕ . The two types of clusters are calibrated differently as the electromagnetic shower starts earlier for electrons than for photons.

After the reconstruction the electron object has to pass more selection criteria to be considered well identified and to reject as much as possible fake contributions.

There are three levels of identification for electrons with different rejection power: loose, medium and tight:

- **Loose** criteria containing cuts on the detector acceptance and the hadronic leakage as well as constraints on the shower shapes in the second sampling of the calorimeter.
- **Medium** criteria stricter than loose, requiring in addition cuts on the first sampling shower shape variables and on the quality of the tracks (number of hits in the Pixels, SCT, and impact parameter).
- **Tight** criteria implying additional identification cuts which test the energy and momentum agreement (E/p) and make use of the TRT detector signal.

Cuts	$E_T > 17 \text{ TeV}$	
	Efficiency (%)	Jet rejection
	$Z \rightarrow ee$	
Loose	87.96 ± 0.07	567 ± 1
Medium	77.29 ± 0.06	2184 ± 13
Tight	61.66 ± 0.07	$(8.9 \pm 0.3)10^4$

Table 1: Electron efficiency for $Z \rightarrow ee$ sample and jet rejection for $p_T > 17 \text{ GeV}$ ³.

On top of these requirements, constraints on calorimetric and track isolation can be used. The efficiency of identification criteria is given in Tab. 1, together with the corresponding rejection power against jets.

3 The $H \rightarrow ZZ^* \rightarrow 4e$ channel analysis

Figure 1 shows the branching ratio for the different Higgs boson decay channels. The experimental limit on the Higgs boson mass given by LEP is 114.4 GeV at 95% C.L. As the Higgs boson couples preferentially to heavy particles, at low mass the privileged decay mode is to $b\bar{b}$; this is a challenging final state to reconstruct in the pp hadronic environment. The $H \rightarrow \gamma\gamma$ decay opens at low mass. Even if the branching ratio is small, this channel has a very clear signal of two isolated photons that makes easier its identification. This channel is a leading channel for low Higgs boson mass. Then the $H \rightarrow ZZ^* \rightarrow 4l$ channel starts to rise, with a branching ratio increasing with m_H . Around 160 GeV this branching ratio drops as the $H \rightarrow W^+W^-$ channel opens up. The backgrounds to the $H \rightarrow ZZ^* \rightarrow 4l$ signal are:

- the irreducible background $ZZ^* \rightarrow 4l$ giving exactly four real leptons in the final state.
- the reducible backgrounds: $Zb\bar{b}$, $t\bar{t}$ and inclusive $Z \rightarrow ee + jets$, giving a similar final state through either semi-leptonic decay of heavy quarks or fake electrons from jets. Requiring lepton isolation squeezes down the amount of this background.

The baseline analysis for reconstructing the $H \rightarrow ZZ^* \rightarrow 4l$ signal proceeds as follows:

- An initial preselection is applied. Events are chosen to have at least four leptons with transverse momentum $p_T > 7 \text{ GeV}$ falling within the pseudorapidity range $|\eta| < 2.5$. Two of these electrons must have $p_T > 20 \text{ GeV}$

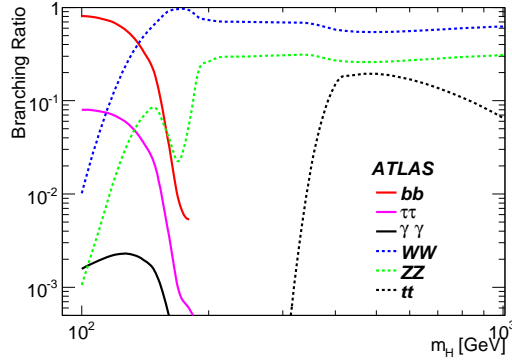


Figure 1: Branching ratio of the different decay modes of the Standard Model Higgs boson as a function of the possible boson mass.

- Then lepton quality cuts are applied: for electron the "medium" quality is requested
- Pairs of leptons of the same flavor and opposite charges are selected, a first one to form the invariant mass the closest to the Z mass, the second one with the highest possible invariant mass.
- Isolation cuts on the leptons are required to remove electrons from jets or b and t quarks decays.
- A cut on the impact parameter on the tracks of the two lower p_T leptons is required to reject the reducible backgrounds. Electrons coming from the Higgs boson decay originate from a vertex close to the interaction point whereas electrons for b and t decays come from vertices displaced from the interaction point. Therefore the impact parameter is an important variable to discriminate between signal and background.
- The four lepton invariant mass is computed.

Table 2 shows the selection efficiency for a Higgs boson with mass of 130 GeV at the different steps of the analysis. Figure 2³ shows the four lepton invariant mass for several different possible

Selection cut	Efficiency for 4e signal (%)
Trigger selection	94.7
Lepton preselection	57.0
Lepton quality and p_T	24.7
Z 's mass cuts	17.1
Calo Isolation	17.1
Tracker Isolation	16.5
Impact Parameter cut	15.1
H mass cut	12.5±0.3

Table 2: Selection efficiency for a Higgs boson of 130 GeV mass analysis.

Higgs boson masses simulated at 14 TeV and 30 fb⁻¹. One can see that the importance of the backgrounds varies with the Higgs boson mass. The $Zb\bar{b}$ and $t\bar{t}$ contributes only in the low mass region and remains a small fraction of the signal. The rejection of such events relies mainly on isolation performances. The irreducible ZZ^* background is by far the dominant background. It becomes maximal around 180 GeV when both Z bosons are real. In this region the signal may be more difficult to extract from background than for lower mass. For higher mass this irreducible background remains important as the Higgs boson invariant mass resolution is getting larger.

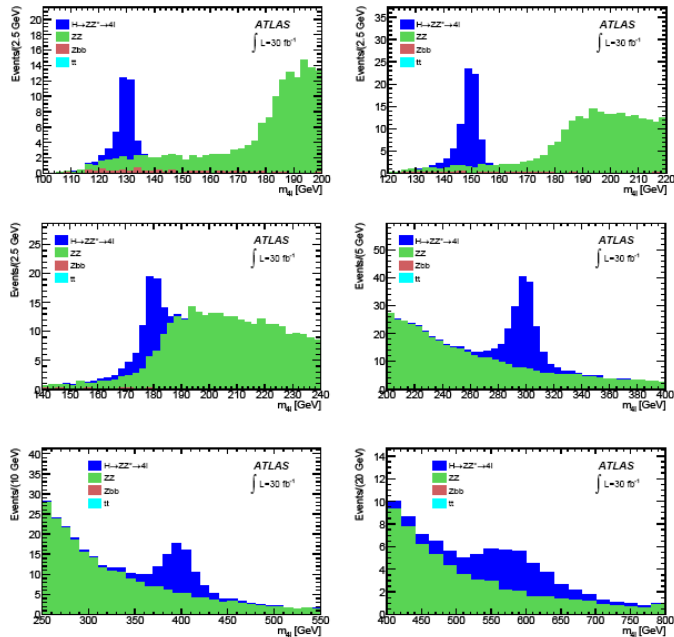


Figure 2: Four leptons invariant mass for signal and backgrounds for different possible Higgs boson masses simulated: 130, 150, 180, 300, 400 et 600 GeV.

4 The electron reconstruction optimization

Since the results given in the first section were published in³ the electron reconstruction has been optimized both for the cluster search and the cluster-track matching. For the cluster search, the seed transverse energy threshold has been lowered to 2.5 GeV and accompanied by a better duplicate cluster rejection. For the cluster-track match an E/p requirement was removed, now keeping the best match in η and ϕ and giving priority to tracks with hits in the pixel and silicon layers over TRT-only tracks (which display poor resolution in η).

For nearly 5% of electrons, the reconstructed cluster can also be considered a photon conversion candidate. In order not to make an a priori choice, these clusters are duplicated as both electrons and photons.

The identification cuts have also been optimized in order to harmonize the trigger and offline selection, and as well to increase the discrimination between signal and backgrounds starting from low momentum (5 GeV). This optimization makes the loose selection stricter. Medium cuts have been loosened to allow for the expected uncertainties on the exact amount of material before the calorimeter during the first ATLAS operating period. Moreover, new more discriminating variables have been introduced. All cuts have been tuned in bins of transverse momentum and pseudorapidity, taking into account the correlations of one with respect to each other. The binning in pseudorapidity follows the expected steps in the material distribution. This optimization has led finally to an efficiency improvement of 12% at medium level for $\eta < 2.5$ and $p_T > 17$ GeV while maintaining the same rejection power. The efficiency of the various cuts is given Tab. 3.

Figure 3 shows the efficiency of the three selection menu levels as function of η and p_T . The overall efficiency has been stabilized as a function of η for loose and medium cuts. For the tight criteria, the losses are caused by the deterioration of the electron reconstruction as the amount of material in front of the calorimeter increases. This affects the stricter cluster-track matching required by the tight criteria, especially at low transverse momenta and high pseudorapidity.

Cuts optimized	$E_T > 20$ TeV	
	Efficiency (%)	Jet rejection
	$Z \rightarrow ee$	
Loose	94.30 ± 0.03	1066 ± 4
Medium	89.97 ± 0.03	6821 ± 69
Tight	71.52 ± 0.03	$(1.38 \pm 0.06)10^5$

Table 3: Electron efficiency for $Z \rightarrow ee$ sample and jet rejection for $p_T > 20$ GeV with the optimized reconstruction.

Although all the range in η and p_T is improved, the main effects of the optimization concern high η region.

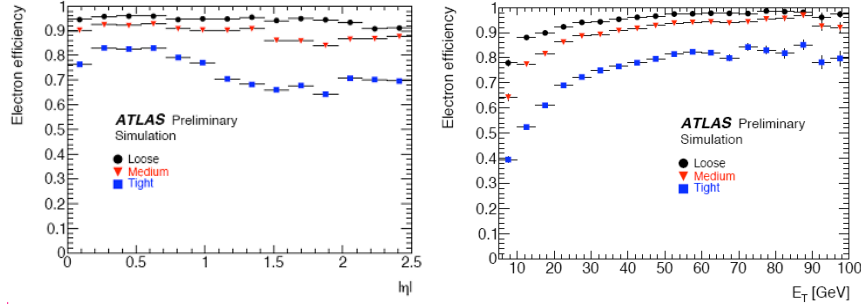


Figure 3: Electron reconstruction efficiencies after optimization as a function of p_T and η .

5 Conclusion

The Higgs to four electron channel is a very promising channel to discover the Higgs boson for mass above 130 GeV thanks to its clear signature of four isolated electrons inside the detectors. The final state reconstruction depends crucially on the electron identification efficiency. A major effort has been performed to optimize the used variables in order to increase the electron reconstruction efficiency keeping a high rejection power against fakes originated from jets. This study led to a 12% efficiency gain at the medium selection for $p_T > 20$ GeV, used for the Higgs to four electron analysis. As sub-leading electrons in the Higgs to four electron channel as a lower p_T in average, a significant gain of about less than $(1.12)^4$ is therefore expected as far as the Higgs signal is concerned. The corresponding precise analysis is currently under study.

References

1. 2008 JINST 3 S08003, The ATLAS Experiment at the CERN Large Hadron Collider, The ATLAS Collaboration, G Aad et al
2. ATLAS detector and physics performance. Technical design report. The Atlas Collaboration. Vol. 1. CERN-LHCC-99-014
3. Expected performance of the ATLAS experiment: detector, trigger and physics. arXiv:0901.0512 The Atlas Collaboration. CERN-OPEN-2008-020
4. CDF and D0 Collaborations, Combined CDF and DZero Upper Limits on Standard Model Higgs-Boson Production with up to 4.2 fb $^{-1}$ of Data, Presented at 44th Rencontres de Moriond: Very high energy phenomena in the universe, La Thuile, Italy, 1-8 feb 2009, Arxiv:0903.4001 [hep-ex]